

MOLECULAR DYNAMICS SIMULATIONS OF GRAPHITE -> DIAMOND TRANSFORMATIONS AND SiC GROWTH ON Si(001)

M. Kitabatake

Central Research Labs., Matsushita Electric Ind., Moriguchi, Osaka 570, Japan.

Direct transformation of graphite to diamond and SiC heteroepitaxial growth on Si(001) were studied by molecular dynamics simulations using the Tersoff potentials of carbon and silicon. The carbon lattice of graphite was compressed along *c*-axis and graphite -> diamond transformations were observed after lattice relaxations. Hexagonal diamond and cubic diamond were synthesized from graphite without any large atomic displacements. Heteroepitaxial growth of single crystal 3c-SiC on Si(001) was observed after carbonization of the Si (001) surface. Breaking of the Si-Si bonds and shrinkage of the [110] Si rows with C atoms are possible mechanisms for the heteroepitaxial growth of SiC on Si(001).

1. INTRODUCTION

We have used molecular dynamics (MD) simulations to understand microchemistry and microstructure of the material syntheses and thin film growth[1-4]. MD simulations enable us to follow atomic trajectories and configurational changes in the processes. In this paper, mechanisms of direct transformation of graphite to diamond and SiC heteroepitaxial growth on Si(001) were studied at atomic scale using MD simulations.

The simulations were carried out using the Tersoff many-body empirical potential for Si and C[5]. The positions and velocities of every atom in the computational cell were calculated following each time step by integrating the equations of motion using the Schofield algorithm[6]. The potential energies and forces associated with each atom in the computational cell, as well as the total potential energy and maximum force value, were calculated for each time step and atomic configurations were allowed to relax. The calculations were carried out using MD and quasidynamic (QD) techniques[2]. The position and velocity of each atom were computed in a fully dynamic mode until both the total potential energy and the total force of the ensemble (independently) reached minima at which point the velocity of each atom was set to zero. The system allowed to evolve further. The procedure was repeated until stable atom positions with approximately zero net

force were obtained. After the QD relaxations, initial unstable configurations changed to more stable configurations which corresponded to a local potential energy minimum.

2. GRAPHITE -> DIAMOND TRANSFORMATIONS

Direct transformation of graphite (G) to diamond (D) has been reported using explosive shock compression[7,8] and static high pressure methods[9]. Cubic diamond (cD) and/or hexagonal diamond (hD) was synthesized by these methods. Several models of mechanisms of these direct transformation of G->D was proposed [8]. Nevertheless a model of G->cD included unreasonable 60 degrees rotation or long slip of the (0001)_G planes. Another model of direct transformation of G->cD was initiated by rhombohedral graphite (rG) which was contained few % in natural graphite. Figure 1 shows these conventional models of G->cD.

Direct transformations of G->hD and G->cD are discussed using the MD and QD simulations. The carbon lattice of graphite was compressed along [0001]_G axis. Small slip of the (0001)_G plane and small displacement of each atom in the (0001)_G plane were introduced to the initial configurations of the QD relaxations. Direct transformation of G->hD and G->cD were observed. Mechanisms of these G->D transformations were illustrated in Fig. 2.

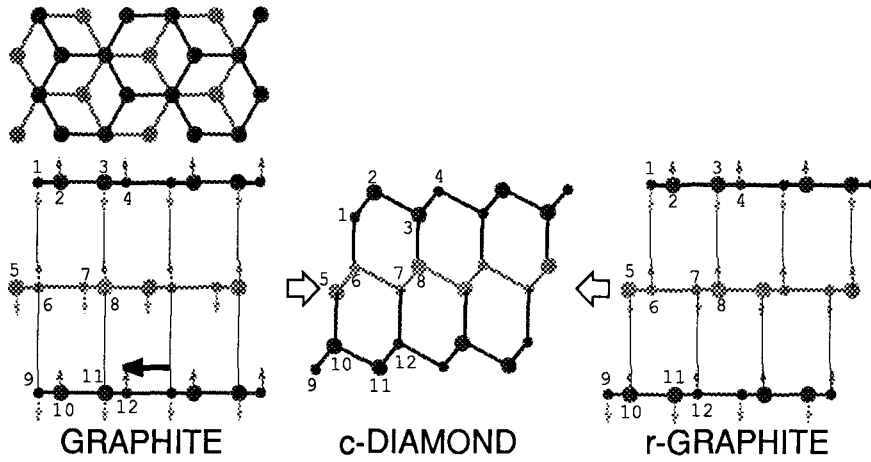


Figure 1. Conventional models of G->cD direct transformations.

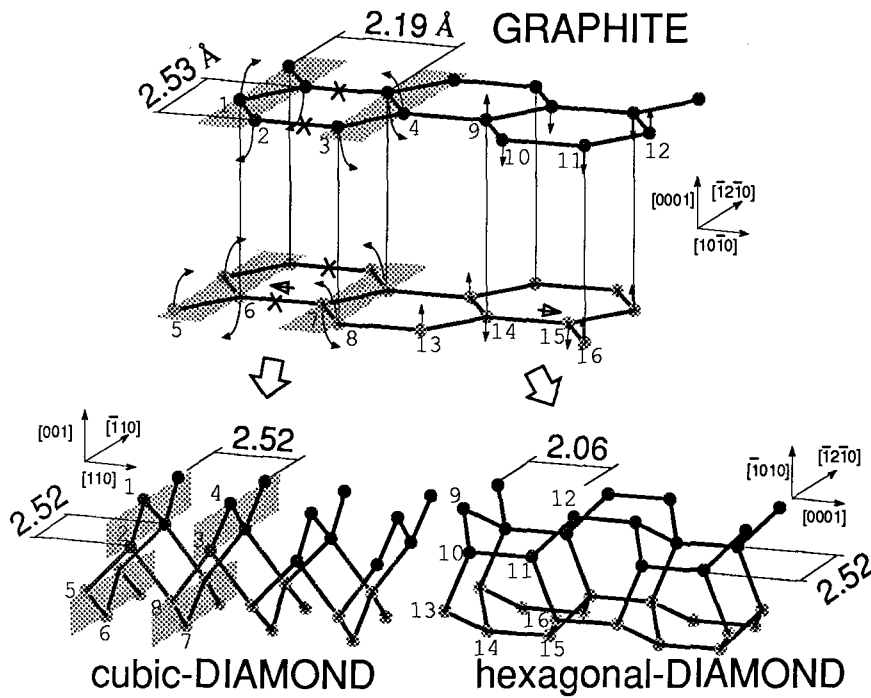


Figure 2. Models of G->hD and G->cD direct transformations proposed using the MD and QD simulations.

2.1. MD simulations of G->hD

G->hD was observed when the QD relaxation was simulated using the initial configurations as follows. The (0001)_G plane spacing of 3.35Å was compressed to the (1010)_{hD} plane spacing of 2.18Å. Small displacements of 0.05Å perpendicular to the (0001)_G planes were introduced to the atoms in the directions of the small arrows in Fig. 2. Lower (0001)_G plane was slipped 0.5Å in the [1010]_G direction as illustrated by large arrow in Fig.2.

After the relaxation, lower (0001)_G plane slipped along the arrow and atoms 9,12,13,16 displaced in the [0001]_G direction. Upper plane atoms 10 and 11 made bonds with lower plane atoms 13 and 16, respectively. Relationships of the crystal axes between G and hD and the stable atomic spacings (Å) in each configurations were

$$[0001]_G/[1010]_{hD} : 3.35 / 2.18 \quad (1),$$

$$[1210]_G/[1210]_{hD} : 2.53 / 2.52 \quad (2),$$

$$[1010]_G/[0001]_{hD} : 2.19 / 2.06 \quad (3).$$

This mechanism of G->hD transformation agrees with the reported conventional models[8].

2.2. MD simulations of G->cD

On the other hand, G->cD was observed when the QD relaxation was simulated using the initial configurations as follows. The (0001)_G plane spacing of 3.35Å was compressed to 2.18Å. Small displacements of 0.1Å perpendicular to the (0001)_G planes were introduced to the atoms in the directions of the small arrows in Fig. 2. No slip of the (0001)_G plane was introduced.

After the relaxation, lower (0001)_G plane slipped along the arrow (opposite direction to that of the G->hD) and atoms 1,4,5,8 displaced in the [0001]_G direction. The bonds 2,3 and 6,7 were broken. The shaded parts of the (0001)_G plane changed to the plane perpendicular to the initial (0001)_G plane. Lower plane atom 8 made bonds with upper plane atoms 2 and 3. Relationships of the crystal axes between G and cD and the stable atomic spacings in each configurations were

$$[0001]_G/[001]_{cD} : 3.35 / 1.78 \quad (4),$$

$$[1210]_G/[110]_{cD} : 2.53 / 2.52 \quad (5),$$

$$[1010]_G/[110]_{cD} : 2.19 / 2.52 \quad (6).$$

This mechanism of G->cD transformation is different from the conventional models.

2.3. Discussions

Experimental studies suggested that the axes relationship $[1210]_{hD}/[110]_{cD}$ of the synthesized diamond and syntheses of the fiber structure along the $[1210]_{hD}$ direction by the shock compression.

In our models, cD and hD synthesized by the direct transformation of G exhibited relationships of (2) and (5). This result suggests the relationship of $[1210]_{hD}/[110]_{cD}$ which agrees with the experimental results. The difference of the lattice spacing between G and D in the G->D transformations were small (<1%) along the $[1210]_G$ direction and large (>13% for cD, >5% for hD) along the $[1010]_G$ direction. These differences of the lattice spacings may cause the syntheses of the fiber structure along $[1210]_{hD}$.

New G->cD mechanism without unreasonable rotations or displacements is proposed by the MD simulations.

3. SiC GROWTH ON Si(001)

Heteroepitaxial growth of cubic silicon carbide (3c-SiC; β-SiC) on Si wafers has been investigated and the surface reaction (carbonization) of a single crystal Si wafer with gaseous hydrocarbons at elevated temperature is essential to grow epitaxial single crystal 3c-SiC thin films[10]. In this paper, the mechanism of the carbonization of the Si(001) surface is studied at atomic scale using the MD and QD simulations.

3.1. MD simulations

36 carbon adatoms were deposited on the surface of the Si lattice whose dimension was 10x10x8 and the configurational change after the QD relaxation was studied.

Figure 3 shows atomic configurations of the relaxed Si(001) surface with the C adatoms after 15000 steps of QD calculations. In the carbonized region, the [110] rows of the (001) surface Si atoms shrink in the [110] direction with C atoms. The side view of the third [110] Si-C row from the top in Fig. 3 (a) is shown in Fig. 3(b). It is clearly observed that the Si surface layer atoms are pulled by the C atoms in the [110] direction to form bonds of Si-C. Some of the Si surface layer

atoms (for example; atom 1 and 2) are unconnected from the second layer Si atoms (3, 4 and 5,6, respectively). The breaking of the Si-Si bonds between first and second layers enables the shrinkage of the [110] row of Si surface atoms with C atoms in the direction of [110]. Si atom 1 is displaced along the arrow in Fig. 3(a),(b) by C atom α and makes new bonds with Si atoms 5 and 6 while atom 1 initially has bonds with Si atoms 3 and 4.

Two-layer 2-dimensional configurations of Si and C (Fig. 3 (b)) correspond to the 3c-SiC configurations whose crystal directions are 3c-SiC[001]//Si[001] and 3c-SiC[110]//Si[110]. This directional relationship between epitaxial 3c-SiC and the Si substrate agree with reported experimental results[10]. Five atom spacings of carbons in the SiC configurations coincide with four atom spacings of the Si lattice as illustrated by vertical lines in Fig. 3(b). This relationship agrees with the bond length ratio of the crystalline lattice; Si/SiC = 2.35/1.89 \approx 5/4. Possible heteroepitaxial growth mechanisms of 3c-SiC on the Si(001) surface are elucidated by the MD simulation as the breaking of the Si-Si bonds between first and second layer atoms in the Si lattice and the shrinkage of the [110] row of the Si lattice atoms with the C atoms.

REFERENCES

1. M.Kitabatake, P.Fons, and J.E.Greene;
J. Vac. Sci. Technol. **A8** (1990) 3726 .
2. M.Kitabatake, P.Fons, and J.E.Greene;
J. Vac. Sci. Technol. **A9** (1991) 91 .
3. M.Kitabatake and J.E.Greene;
J. Appl. Phys. **73** (1993) 3183.
4. M.Kitabatake, M.Deguchi, and T.Hirao;
J. Appl. Phys. to be published (1993).
5. J.Tersoff; Phys.Rev. **B39** (1989) 5566.
6. P.Schofield; Comp.Phys.Comm. **5** (1973) 17.
7. L.F.Trueb; J.Appl.Phys.**39**(1968) 4707.
8. E.J.Wheeler and D.Lewis;
Mat. Res. Bull. **10** (1975) 687.
9. F.P.Bundy; J.Chem.Phys. **38** (1963) 631.
10. K.Shibahara, S.Nishino, and H.Matsunami;
J. Crystal Growth **78**, 538 (1986).

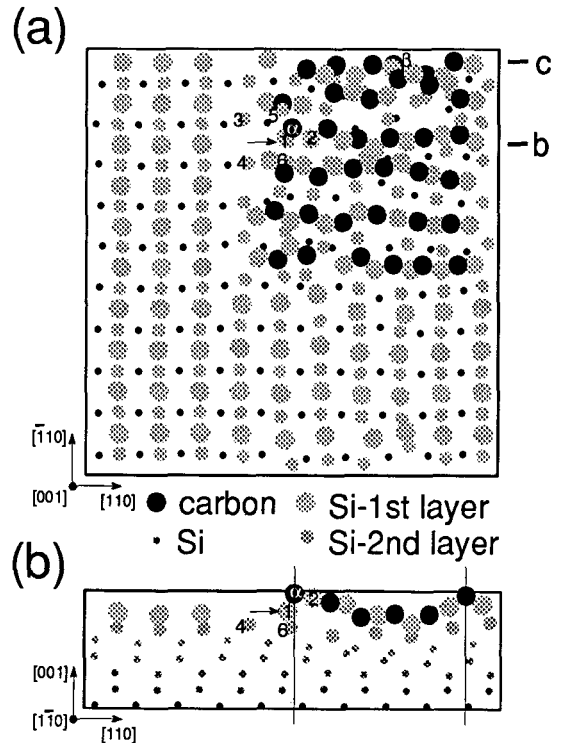


Figure 3. Atomic configurations of the relaxed Si(001) surface with the adsorbed C atoms after 15000 steps of the QD calculation.

(a) top view.

(b) side view of the third [110] Si-C row from the top in (a) (b-plane in (a)).